ELSEVIER

Journal of Food Engineering 60 (2003) 453–462

JOURNAL OF FOOD ENGINEERING

www.elsevier.com/locate/jfoodeng

On the thermal inertia of the wall of a drum dryer under a cyclic steady state operation

M. Kostoglou [a,b,*], T.D. Karapantsios [a,c]

[a] *Food Process Engineering Laboratory, Department of Food Technology, Technological Educational Institution of Thessaloniki, P.O. Box 14561, 54101 Thessaloniki, Greece*

[b] *Chemical Process Engineering Research Institute, P.O. Box 1517, 54006 Thessaloniki, Greece*

[c] *Department of Chemistry, Division of Chemical Technology, Aristotle University of Thessaloniki, Box 116, 54124 Thessaloniki, Greece*

Received 15 February 2002; accepted 25 February 2003

Abstract

A mathematical framework is developed for studying the heat transfer through the metallic wall of an internally heated rotating drum of a drum dryer. Contrary to the few earlier analyses that solved numerically the transient two-dimensional partial differential equation of heat conduction until a cyclic steady state is reached, the present analysis transforms it to a one-dimensional integral equation that can be solved directly for the cyclic steady state. In this new formulation the thermal inertia of the wall is directly assigned to specific terms of the kernel of the integral equation which makes the assessment of its contribution very easy. A numerical method for the solution of the integral equation is developed. An approximate solution method based on polynomial expansion is developed, too. Results from the different solution approaches of the effect of thermal inertia on the response of the dryer are discussed for both simplified and realistic cases.

Keywords: Thermal inertia; Cyclic steady state; Integral equation approach; Drum drying

1. Introduction

The use of drum dryers is a common industrial practice for the production of a variety of foodstuffs such as yeast creams, fruit purees, baby foods, mashed potatoes, dry soup mixtures, pregelatinized starches etc (Bonazzi et al., 1996; Moore, 1995). This type of drying is suitable for products which are viscous in their natural state or after concentration and as such they are better dried in the form of very thin films (Falagas, 1985).

The most common type of this dryer consists of a drying cylinder (drum) mounted on a horizontal axis and mechanically rotated with variable speed control. The drum is heated by steam condensing on its inside surface, the drying effect being obtained by the transfer of heat from the inside of the drum through its metallic wall to a film of material spread over its external surface. Different methods have been employed in the past to apply the material as a film over the drum surface depending chiefly on the product's rheological properties. Spreading by submersion, by atomization, by auxiliary non-heated small rollers, by using a twin-drum or a double drum arrangement are among the most popular drum dryer configurations. Gardner (1971) and Moore (1995) have presented useful accounts on this topic. Whatever the spreading method, the applied film is no longer in motion relative to the drum because of rapid drying and solidification. After travelling part of a revolution, the dried material is removed in the form of thin sheets by scraper knifes (doctor blades).

Theoretical modeling of the drum drying process is very important for the design, optimization and control of drum dryers. Yet, it is a very difficult task since drum drying is a really complex process requiring except for a submodel of the drying process itself, a fluid dynamics submodel (for initial film deposition over the drum) and a heat transfer submodel (heat conduction through the drum solid wall). Trystram and Vasseur (1992) have shown in detail how the different submodels can be

* Corresponding author. Address: Food Process Engineering Laboratory, Department of Food Technology, Technological Educational Institution of Thessaloniki, P.O. Box 14561, 54101 Thessaloniki, Greece.

E-mail addresses: kostoglu@cperi.certh.gr (M. Kostoglou), karapant@cperi.certh.gr (T.D. Karapantsios).

0260-8774/$ - see front matter © 2003 Elsevier Ltd. All rights reserved.
doi:10.1016/S0260-8774(03)00076-1

effectively integrated in a global dryer model. The drying submodel has been extensively studied by Vasseur and co-workers (Abchir, Vasseur, & Trystram, 1988; Trystram, Meot, Vasseur, Abchir, & Couvrat-Desvergnes, 1988; Trystram & Vasseur, 1992; Vasseur, Kabbert, & Lebert, 1991b) and Daud and Armstrong (1987, 1988). The fluid dynamics submodel has been examined by Daud (1986). A recent contribution on this issue has been presented by Vallous, Gavrielidou, Karapantsios, and Kostoglou (2002). The focus of the present work is on the heat transfer submodel.

Earlier studies did not realize the role of the thermal inertia of the drum wall in the dryer's heat transfer performance. Fritze (1972, 1973a, 1973b), analyzed the drum dryers' thermal efficiency in terms of overall heat transfer coefficients, an approach which assumes a stationary (around the drum circumference) steady state conduction through the drum metallic wall. Kozempel, Sullivan, Craig, and Heiland (1986) developed a simple model based also on the assumption of stationary steady state heat fluxes through the drum wall. As a result, the outside temperature of the drum was taken not only constant in every angular position of the drum but also equal to the temperature of the condensing steam which is by far not true (e.g., Abchir et al., 1988; Vasseur, Abchir, & Trystram, 1991a).

Daud and Armstrong (1987) relaxed the earlier approximation of steady state heat fluxes by taking the thermal resistance of the drum wall into account and divided the dryer into three angular zones with different heat and mass transfer characteristics. However, the great significance of the thermal inertia of the wall to realistically model heat transfer in a drum dryer was shown first by Abchir et al. (1988) and was further supported by Vasseur, Abchir, and Trystram (1991a) and Trystram and Vasseur (1992). Recently, Karapantsios and co-workers (Anastasiades, Thanou, Loulis, Stapatoris, & Karapantsios, 2002; Gavrielidou, Vallous, Karapantsios, & Raphaelides, 2002; Kalogianni, Xinogalos, Karapantsios, & Kostoglou, 2002; Vallous et al., 2002; Vlachos & Karapantsios, 2000) communicated the results of a large experimental campaign (1997–2000) conducted on an industrial scale drum dryer. These studies used modern instrumentation and data analysis techniques to investigate the complex phenomena governing the performance of a drum dryer. This work is a step further, aiming to study the heat transfer submodel of the drum dryer from a mathematical point of view.

First, the mathematical problem is formulated in a way that permits direct evaluation of the various physical properties and operational parameters that have a significant contribution on the response of the system. Next, several solution approaches are given in detail. These solutions are compared for accuracy and consistency in a case of a simplified drying submodel since the latter has no influence on the basic features of the heat transfer submodel. Typical results from the different solution approaches are cross-examined for a few more realistic cases. Possible extension of the proposed solution procedure to include terms such as heat losses to the environment, a spatially variable Biot number at the inside of the drum and a more realistic drying model are discussed.

2. Problem formulation and solution

The temperature distribution $T(z,y)$ inside the drum wall is given from the solution of the following equation:

$$u\rho c_p \frac{\partial T}{\partial z} = k\frac{\partial^2 T}{\partial y^2} \tag{1}$$

where y is the coordinate across the drum wall and z is a length coordinate measured from the point (moment) of material application as a film over the drum and it is associated with time through the relation $\mathrm{d}z/\mathrm{d}t = u$ (u is the velocity of the wall). Nissan and Hansen (1960) presented the exact derivation of Eq. (1) with the appropriate boundary conditions (BCs):

at $y = 0$ (inner side of drum)

$$-k\frac{\partial T}{\partial y} = h(T_\mathrm{v} - T) \tag{2}$$

at $y = w$ (outer side of drum)

$$-k\frac{\partial T}{\partial y} = Q(T,X) \quad \text{for } iL < z < iL + L_1 \tag{3a}$$

$$\frac{\partial T}{\partial y} = 0 \quad \text{for } iL + L_1 < z < (i+1)L \tag{3b}$$

where T_v is the steam temperature, h is the steam-side heat transfer coefficient (assumed constant for all z) and k, ρ and c_p are the thermal conductivity, density and specific heat of the solid wall, respectively. Also, X is the moisture content of the drying material (kg H_2O/kg dry solid), w is the wall thickness, L is the length of a full rotation, L_1 is the part of the revolution covered with drying material and i is an index which denotes the number of full rotations from the moment of initial material application. Eq. (3a) couples the heat transfer problem through the drum wall with the drying process of the material spread over the external surface of the drum. X is given from the solution of the following ordinary differential equation (ODE):

$$u\Delta H C_\mathrm{s}\frac{\mathrm{d}X}{\mathrm{d}z} = -Q(T,X) \quad \text{for } iL < z < iL + L_1 \tag{4}$$

where ΔH is the latent heat of water evaporation and C_s is the so-called specific load (kg dry solid/m^2).

The initial conditions are a prescribed value of temperature for $z = 0$, $T(0,y) = T_0(y)$, and a prescribed value of moisture at the start of each cycle (rotation),

$X(iL) = X_0$. In the case where only the steady state cyclic operation is of interest the index i in the above equations can be disregarded since the temperature is periodic with respect to z with period L and the temperature initial condition must be substituted with $T(0,y) = T(L,y)$.

The following non-dimensionalization is introduced next:

$$z = \frac{kz}{w^2 u \rho c_p} \quad Bi = \frac{hw}{k} \quad Q = \frac{Qw}{kT_v} \quad y = \frac{y}{w}$$

$$p = \frac{L_1}{L} \quad L = \frac{kL}{w^2 u \rho c_p} \quad X = \frac{X}{X_0} \quad T = \frac{T_v - T}{T_v}$$

$$D = \frac{\rho c_p w T_v}{\Delta H C_s X_0}$$

To keep the notation simple, some dimensionless variables retain the symbol of their dimensional counterpart. This is not confusing since in the rest of the present work only dimensionless variables will be invoked.

Now the problem which must be solved takes the form

$$\frac{\partial T}{\partial z} = \frac{\partial^2 T}{\partial y^2} \tag{5}$$

with BCs

at $y = 0$

$$\frac{\partial T}{\partial y} = Bi\, T \tag{6}$$

at $y = 1$

$$\frac{\partial T}{\partial y} = Q(T,X) \quad \text{for } iL < z < (i+p)L \tag{7a}$$

$$\frac{\partial T}{\partial y} = 0 \quad \text{for } (i+p)L < z < (i+1)L \tag{7b}$$

$$\frac{dX}{dz} = -DQ(T,X) \quad \text{for } iL < z < (i+p)L \tag{8}$$

and initial conditions $X(iL) = 1$ and $T(0,y) = T_0(y)$.

The solution of the above problem can be written in the following integral form

$$T(y,z) = \int_0^1 G(z,y;0,y') T_0(y')\, dy' + \int_0^z G(z,y;z',1) \left(\frac{\partial T}{\partial y} \right)_{y=1} dz' \tag{9}$$

where the Green's function $G(z,y;z',y')$ is given from the solution of the following equation

$$\frac{\partial G}{\partial z} = \frac{\partial^2 G}{\partial y^2} + \delta(z - z')\delta(y - y') \tag{10}$$

with the BCs

$$\frac{\partial G}{\partial y} = Bi\, G \quad \text{at } y = 0 \tag{11}$$

$$\frac{\partial G}{\partial y} = 0 \quad \text{at } y = 1 \tag{12}$$

where the symbol delta denotes the Dirac delta function.

Eq. (10) can be solved as follows: first, the source term (delta functions) is disregarded and the remaining homogeneous partial differential equation (PDE) is solved using the separation of variables technique. The general solution of the homogeneous equation is given as

$$G = \sum_{i=1}^{\infty} \alpha_i e^{-\lambda_i^2 z} \frac{X_i(y)}{F} \tag{13}$$

where the eigenvalues λ_i are the roots of the following transcantental equations

$$\lambda_i \tan(\lambda_i) = Bi \tag{14}$$

N is the normalization factor given from

$$F^2 = \int_0^1 X_i^2(y)\, dy \tag{15}$$

and the eigenfunctions X_i have the form

$$X_i(y) = \sin(\lambda_i y) + \frac{1}{\tan(\lambda_i y)} \cos(\lambda_i y) \tag{16}$$

Next, the source term in Eq. (10) is expanded in a series of the eigenfunctions X_i using the properties of the orthogonal functions. Then, by equating this expansion with the series (13), the unknown coefficients α_i of (13) are found. Finally, the Green's function is determined as:

$$G(z,y;z',y') = \sum_{i=1}^{\infty} \frac{1}{F^2} e^{-\lambda_i^2 (z - z')} X_i(y) X_i(y') \tag{17}$$

Eq. (9) is not amenable to an analytical solution since the temperature distribution with respect to y for $z = 0$ appears in its right hand side. In order to get rid of this, lets assume the case for which the initial (with respect to drying) temperature of the drum is equal to that of the vapor. This is a quite realistic assumption since it is already assumed that the losses to the environment are negligible and so by starting the vapor flow, the drum after some time will reach the vapor temperature. The drying process starts the moment the drying material is applied over the drums for the first time (assumed to happen instantaneously) and this is considered the beginning of time ($z = 0$). After some transient period of several revolutions the system will finally reach a cyclic steady state. This scenario offers a convenient way to develop the direct solution for the cyclic steady state.

The initial condition of the drum temperature being equal to the vapor temperature means that $T_0(y) = 0$, so the first term of the right hand side of Eq. (9) is eliminated. The remaining equation combined with Eqs. (7a) and (7b) demonstrate that the temperature anywhere inside the drum shell can be determined provided that

the temperature of the outer drum surface is known. In this way, the 2D initial problem is reduced to the 1D problem of finding the outer surface temperature. Writing Eq. (9) for the outer surface temperature yields:

$$T(z,1)=\int_0^z g(z;z')\left(\frac{\partial T}{\partial y}\right)_{y=1}\mathrm{d}z' \tag{18}$$

where the kernel function $g(z;z')$ is the Green's function $G(z,1;z',1)$ and has the following explicit form

$$g(z;z')=\sum_{i=1}^{\infty} d_i\,\mathrm{e}^{-\lambda_i^2(z-z')} \tag{19}$$

where

$$d_i=\left[\sin(\lambda_i)+\frac{\cos(\lambda_i)}{\tan(\lambda_i)}\right]^2\left[\left(\frac{1}{2}-\frac{\sin(2\lambda_i)}{4\lambda_i}\right)+\frac{1}{\tan^2(\lambda_i)}\left(\frac{1}{2}+\frac{\sin(2\lambda_i)}{4\lambda_i}\right)+\frac{\sin^2(\lambda_i)}{2\lambda_i\tan(\lambda_i)}\right]^{-1} \tag{20}$$

For the ease of presentation, the outer surface temperature of the drum is denoted by T_e (i.e $T_\mathrm{e}(z)=T(z,1)$). Substitution of the BC (7a) to Eq. (18) and splitting of the integral per period leads to the following integral equation:

$$T_\mathrm{e}=\sum_{j=0}^{i-1}\int_{jL}^{jL+pL} g(z;z')Q(T_\mathrm{e},X)\,\mathrm{d}z'+\int_{iL}^{iL+z} g(z;z')Q(T_\mathrm{e},X)\,\mathrm{d}z'\quad \text{for } iL<z<iL+pL \tag{21a}$$

$$T_\mathrm{e}=\sum_{j=0}^{i}\int_{jL}^{jL+pL} g(z;z')Q(T_\mathrm{e},X)\,\mathrm{d}z'\quad \text{for } iL+pL<z<iL+L \tag{21b}$$

The above equations are a generalized form of the nonlinear integral Volterra equation and must be solved combined with the ODE for the moisture to find the outer surface temperature evolution. After some initial transient time the drum dryer reaches a steady state periodic operation and the temperature T_e and moisture distribution do not change from cycle to cycle. The solution of the transient equations for the periodic steady state is in general very difficult due to the fact that the transient period may be very long. So, it is highly desirable to find a formulation which admits direct computation of the periodic solutions and avoids transient computations.

Let us assume that the dryer operates for a very long time and the cyclic operation has been already established long ago. This means that the following conditions hold

$$T_\mathrm{e}(z)=T_\mathrm{e}(z+iL) \tag{22a}$$

$$X(z)=X(z+iL) \tag{22b}$$

Eq. (21) apply now to every (new) cycle which is renumbered with $i=0$. All the previous cycles must have the same temperature distribution according to the conditions (22). So, Eq. (21) for the case of a cyclic operation must be transformed to:

$$T_\mathrm{e}=\sum_{j=-\infty}^{-1}\int_{jL}^{jL+pL} g(z;z')Q(T_\mathrm{e},X)\,\mathrm{d}z'+\int_0^z g(z;z')Q(T_\mathrm{e},X)\,\mathrm{d}z'\quad \text{for } 0<z<pL \tag{23a}$$

$$T_\mathrm{e}=\sum_{j=-\infty}^{0}\int_{jL}^{jL+pL} g(z;z')Q(T_\mathrm{e},X)\,\mathrm{d}z'\quad \text{for } pL<z<L \tag{23b}$$

A very interesting observation is that Eq. (23b) gives explicitly the temperature for $pL<z<L$ if just the temperature for $0<z<pL$ is known. This practically means that only the temperature between 0 and pL is unknown and it must be found from the solution of Eq. (23a). To further simplify the situation, the integration limits in (23) are changed (subtraction of jL) and the functions g are substituted from (19) to give:

$$T_\mathrm{e}=\int_0^{pL}\sum_{j=-\infty}^{-1}\sum_{i=1}^{\infty} d_i\,\mathrm{e}^{-\lambda_i^2(z-z')+j\lambda_i^2L}Q(T_\mathrm{e},X)\,\mathrm{d}z'+\int_0^z\sum_{i=1}^{\infty} d_i\,\mathrm{e}^{-\lambda_i^2(z-z')}Q(T_\mathrm{e},X)\,\mathrm{d}z'\quad \text{for } 0<z<pL \tag{24}$$

This equation must be solved together with

$$\frac{\mathrm{d}X}{\mathrm{d}z}=-DQ(T_\mathrm{e},X) \tag{25}$$

So, using the above analysis the two-dimensional PDE (5) which should be originally solved for unbounded time is transformed together with its BCs to the one-dimensional integral equation (24) which must be solved for a specific time interval.

3. Exact solution of the integral equation

For the particular case where the evaporation rate is not a function of temperature and also $Q(T,X)=\alpha X$, the temperature distribution can be obtained analytically as

$$T_\mathrm{e}=\alpha\sum_{j=-\infty}^{-1}\sum_{i=1}^{\infty}\frac{d_i}{\lambda_i^2-\alpha D}\mathrm{e}^{-\lambda_i^2z+j\lambda_i^2L}\left(\mathrm{e}^{(\lambda_i^2-\alpha D)pL}-1\right)+\sum_{i=1}^{\infty}\frac{d_i}{\lambda_i^2-\alpha D}\left(\mathrm{e}^{-\alpha Dz}-\mathrm{e}^{-\lambda_i^2z}\right)\quad 0<z<pL \tag{26a}$$

$$T_\mathrm{e}=\alpha\sum_{j=-\infty}^{0}\sum_{i=1}^{\infty}\frac{d_i}{\lambda_i^2-\alpha D}\mathrm{e}^{-\lambda_i^2z+j\lambda_i^2L}\left(\mathrm{e}^{(\lambda_i^2-\alpha D)pL}-1\right)\quad pL<z<L \tag{26b}$$

4. Numerical solution of the integral equation

In general, the integral equation (24) must be solved numerically. Before speaking about any numerical method, it is apparent that the infinite series in Eq. (24) must be truncated. The significance of the truncation order is discussed next. The inner sum with respect to i has to do with the addition of more eigenfunctions (harmonics) to the solution of Eq. (5). As thermal inertia gets more prominent, the temperature profile inside the drum wall becomes steeper so more terms are needed for the representation of the profile. On the other hand, the outer summation with respect to j has to do with the interaction between the cycles. As thermal inertial increases more cycles must be taken into account in order to find the cyclic solution. In both sums, the truncation must be performed up to high enough values so as not to influence the results of the numerical solution.

The numerical solution of Eq. (24) is by no means trivial. Its structure is equivalent to that of a hyperbolic PDE, so the usual discretization techniques lead to significant dispersion/numerical diffusion errors. In other words, the kernel functions are singular at $z = 0$ (but the singularity is integrable), so direct numerical integration is not possible.

This problem can be overcome as follows: first, a partition $z_i = iH$ is defined on the interval $[0, pL]$, where $i = 0, 1, 2, \ldots, N$ and $H = pL/N$. Let T_{ei}, X_i and Q_i be the values of the corresponding quantities at z_i. The crucial point is the assumption that in the interval (z_i, z_{i+1}), Q equals to $(Q_i + Q_{i+1})/2$. By substituting this in Eq. (24), the integrals for each interval can be evaluated analytically. Additionally, this substitution is equivalent to the trapezoidal rule (second order accuracy as regards integration with respect to Q). The result of the above procedure is $(m = 0, 1, 2, \ldots, N)$

$$T_{em} = \frac{1}{2}\sum_{k=1}^{N} b_{mk}(Q_k + Q_{k-1}) + \frac{1}{2}\sum_{k=1}^{m} c_{mk}(Q_k + Q_{k-1}) \tag{27}$$

where

$$b_{mk} = \sum_{j=-\infty}^{-1}\sum_{i=1}^{\infty}\frac{d_i}{\lambda_i^2}(\mathrm{e}^{-\lambda_i^2 z_m + \lambda_i^2 jL})(\mathrm{e}^{\lambda_i^2 z_k} - \mathrm{e}^{\lambda_i^2 z_{k-1}}) \tag{28a}$$

$$c_{mk} = \sum_{i=1}^{\infty}\frac{d_i}{\lambda_i^2}\mathrm{e}^{-\lambda_i^2 z_m}(\mathrm{e}^{\lambda_i^2 z_k} - \mathrm{e}^{\lambda_i^2 z_{k-1}}) \tag{28b}$$

Eq. (25) is integrated analytically to give

$$X = 1 - D\int_0^z Q\,\mathrm{d}z \tag{29}$$

The discretized form of the above equation using the trapezoidal rule is

$$X_m = 1 - HD\left(\frac{Q_0 + Q_m}{2} + \sum_{k=1}^{m-1} Q_k\right) \tag{30}$$

Finally, the problem is closed by assuming the relation between heat flux and surface temperature with the moisture content which, being evaluated at the discretization points, gives the following set of equations

$$Q_m = Q(T_{em}, X_m) \tag{31}$$

The Eqs. (27), (30) and (31) constitute a system of $3N + 3$ equations which must be solved simultaneously. This can be done easily using an iterative strategy. Starting with an estimation for Q_m, Eqs. (27) and (30) are solved for the computation of T_{em} and X_m, respectively, and then these values are substituted to (31) to give improved values for Q_m. Evidently, the convergence of the above procedure depends on how close is the initial estimation to the required solution. A good initial estimation leads to convergence after few iterations. As the initial estimation becomes poorer, the required number of iterations increases and finally the method diverges. In that case, the Newton–Raphson method must be used for the solution of the problem. The Newton–Raphson method ensures convergence and needs smaller number of iterations than the above direct procedure. The computational cost per iteration is kept low by using the analytically computed Jacobian of the system. The elements of the $(N + 1) \times (N + 1)$ Jacobian are

$$J_{mk} = \delta_{mk} - Q_T(T_{em}, X_m)h_{mk} - Q_X(T_{em}, X_m)e_{mk} \tag{32}$$

where

$$2h_{mk} = (1 - \delta_{k0})b_{mk} + (1 - \delta_{kN})b_{mk+1} + [(1 - \delta_{k0})c_{mk} + (1 - \delta_{kN})c_{mk+1}]U(k - m)$$

$$2e_{mk} = [(2 - \delta_{k0} - \delta_{kN})HD]U(k - m)$$

The subscript X or T of Q denotes partial derivative with respect to the corresponding variable, the symbol δ_{ij} is the Kronecker delta and the function $U(x)$ takes the value 1 for $x \leqslant 0$ and 0 in any other case.

It must be mentioned that the above constitutes an implicit type discretization method so the solution of the problem is stable irrespective of the grid size.

Finally, the temperature T_e for $pL < z < L$ can be computed as

$$T_e = \frac{1}{2}\sum_{k=1}^{N}\sum_{j=-\infty}^{0}\sum_{i=1}^{\infty}\frac{d_i}{\lambda_i^2}(\mathrm{e}^{-\lambda_i^2 z_m + \lambda_i^2 jL})(\mathrm{e}^{\lambda_i^2 z_k} - \mathrm{e}^{\lambda_i^2 z_{k-1}}) \times (Q_k + Q_{k-1}) \tag{33}$$

5. Polynomial (quadratic) approximation

The low order polynomial approximation of the unknown function as a method for the solution of PDEs has a long history in transport phenomena

(Crank, 1975; Ozisik, 1989). This method is much better than neglecting completely the thermal inertia since it permits the development of a temperature profile but due to the low order of the polynomial, the approximation of steep profiles is poor and the method is not appropriate for a very large thermal inertia. The quadratic approximation assumes that the temperature distribution in the drum wall (y-direction) has the following polynomial form

$$T = c_1 + c_2 y + c_3 y^2 \tag{34}$$

where c_i are unknown functions of z which must be determined in order to satisfy (as closely as possible) the BCs and the PDE. The mean temperature T_m across the wall (y-wise) is given by taking the integral of (34) for y from 0 to 1:

$$T_m = c_1 + c_2/2 + c_3/3 \tag{35}$$

Substituting the above in the BC (7b) for the inner wall leads to the following expression:

$$T = T_m + \frac{Bi(T_m - c_3/3)}{1 + \frac{Bi}{2}}(y - 1/2) + c_3(y^2 - 1/3) \tag{36}$$

The integral with respect to y of Eq. (5) with limits at $y = 0$ and 1 after using the BCs leads to

$$\frac{dT_m}{dz} = Q(T(1), X) - BiT(0) \tag{37}$$

where $T(1)$ and $T(0)$ can be found from Eq. (34) by substituting $y = 1$ and 0, respectively. From the above it is obvious that the remaining unknown quantities are the mean temperature T_m, the coefficient c_3 and the moisture content X. The differential equation for X is the following

$$\frac{dX}{dz} = -DQ(T(1), X) \tag{38}$$

By substitution of Eq. (36) to the BC (7a), we end up with the following implicit algebraic equation for c_3

$$\left(2 - \frac{Bi}{3}\left(1 + \frac{Bi}{2}\right)^{-1}\right)c_3 = Q(T(1), X) - BiT_m\left(1 + \frac{Bi}{2}\right)^{-1} \tag{39}$$

The differential–algebraic system of equations (37)–(39) must be integrated numerically in order to obtain the evolution of the temperature distribution. A Runge–Kutta explicit integrator with adaptive step size and prespecified accuracy (Press, Teukolsky, Vetterling, & Flannery, 1992) is used for the differential equations (37) and (38) while (39) is solved for c_3 in each time step by an iterative procedure using the previous step values of c_3 as an initial estimation. Convergence is typically achieved in three or four iterations. The integration is started using a zero initial mean temperature and is continued until the establishment of a cyclic operation.

6. Possible generalizations of the proposed solution procedure

The possibilities of extending the proposed method of solution to include more terms (effects) is discussed next. Before that, it is useful to survey its basic features. After the selection of a particular discretization (which can be non-uniform), the coefficients b_{mk} and c_{mk} can be computed. These coefficients are functions only of L and Bi and not of the drying kinetics $Q(T, X)$, so they can be computed directly (independently of the drying kinetics). After this, the resulting system of algebraic equations is solved using the Newton–Raphson method to find the outer wall temperature in the part of the drum covered with the drying material. The outer wall temperature at the bare surface of the rest of the drum (between the doctor blades and the new material feed point) is computed in a post-processing step.

The present method of solution is developed for the aforementioned idealized case but it can be extended to more realistic cases. A first complexity is to assume a heat loss model (natural convection, radiation) towards the environment. This feature can be easily added to the proposed methodology. The discretization of the whole drum dryer surface is needed and the outer wall temperature results directly from the solution of the algebraic system of equations. A much more difficult case is that of a spatially dependent (in the angular direction) heat transfer coefficient between the vapor and the inner surface of the drum. In practice, this is a quite true situation due to the condensate film flowing down the inner drum wall and also the condensate accumulating at the bottom of the drum. To accommodate a spatially dependent Biot number, considerable new development is required. The Neumann–Neumann–Green functions, which are independent of the Biot number, should be used instead of the Robin–Neumann used in the present analysis. Then two integral equations are constructed which relate the outer with the inner wall surface temperatures. Obviously, in this case both surfaces of the drum dryer wall must be discretized in order to solve for the corresponding temperatures.

Finally, the function $Q(T, X)$ may not be a simple algebraic expression but rather a complicated drying model (e.g. Daud & Armstrong, 1987, 1988). Such a model typically consists of a set of PDEs for heat and mass transfer in a domain with a moving boundary. This model must be solved in combination with the equation of heat transfer in the drum wall. The proposed methodology can be used even in this case. In each iteration for the outer wall temperature, the solution of the drying model is needed. In another approach, the problem to be solved can be restricted to the domain of the material (drying model) by eliminating the wall domain, using Eq. (24) as a BC. This approximation discards also the

explicit time dependency and a steady state (cyclic) problem has to be solved.

7. Results

In a first step, we shall try to examine the influence of the number of terms used in series (28) on the results. The outer sum is truncated to $j = -M$ and the inner one to $i = K$. In order to identify the sensitivity with respect to M and K, the analytical solution will be used since all the basic features of the process are still adequately represented when assuming $Q(T,X) = \alpha X$ and $p = 1$. The parameters for this simple case are L (which can be seen as the Fourier number of the process or alternatively as an inverse rotation frequency) and αDL which denotes how sharp is the heat flux profile. A typical range of the parameter L is between 0.1 and 5 whereas a typical range of αDL is between 3 (slow drying) and 15 (fast drying).

In general, the parameter L dictates the value of M whereas the parameter αDL dictates the value of K which is needed for accurate results. First, the relation between L and M is examined. In Fig. 1, the dimensionless temperature profiles of the outer wall of the drum are shown for several values of M when $L = 0.1$ and $\alpha DL = 3$. Apparently, the $M = 1$ (no thermal inertia) approximation is quite in error and at least $M = 25$ is needed to get an accurate result. In Fig. 2, the value of the outer drum temperature at $z = 0.2L$ is given as a function of M for several values of L. As L increases (rotation speed drops) the number of terms needed for convergence decreases. For $L = 1$, $M = 2$ is enough for an accurate solution and even the zero thermal inertia approximation ($M = 1$) is a rational one. The significance of M is that it denotes the number of cycles over which one must integrate Eq. (1) starting with an initial temperature equal to that of vapor, in order to reach a cyclic steady state.

A typical value $L = 0.5$ is assumed in order to see the effect of the parameter αDL on the number K of i-terms needed for an accurate solution. In Fig. 3, the outer temperature profiles are shown for $\alpha DL = 15$ and for several values of K. The convergence is fast for large values of z and very slow for small values of z (at least $K = 20$ terms are required). This behavior is attributed to the discontinuity exhibited by the flux Q at $z = 0$. It must be stressed though, that unlike the case of a discontinuous temperature at $z = 0$ where the flux exhibits a singularity, here the series solution converges everywhere using a finite number of terms (even for $z = 0$). In Fig. 4, the temperature at $z = (4/50)L$ is shown as a function of the number of inertial terms K and for several values of αDL. It is interesting that the convergence is not improved as the drying gets slower. This is because the key contribution to thermal inertia emerges from the sudden onset of drying and not from the slope of the drying curve.

The above results refer to the case of no heat transfer resistance between the condensing steam and the internal drum surface ($Bi = \infty$). The question now is how the Biot number influences the convergence properties of the solution. In general, as Biot decreases the temperature profile across the wall thickness becomes more uniform, so the number of eigenfunctions (K), which is needed to accurately represent it, decreases. On the

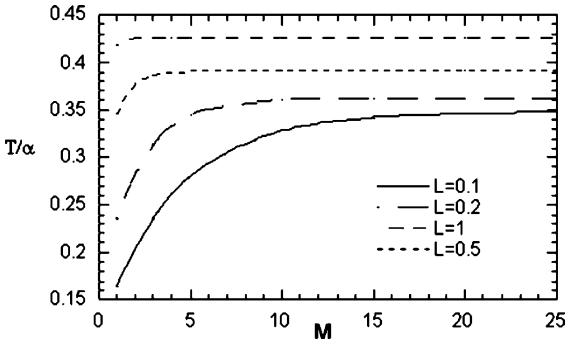

Fig. 2. Dimensionless outer surface temperature versus M (bound of index j) for several values of L. Analytical solution.

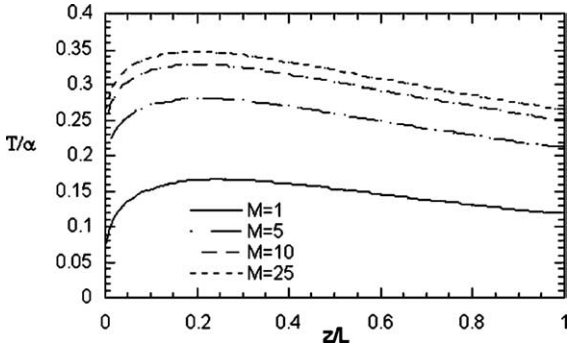

Fig. 1. Dimensionless outer surface temperature along the drum for several values of M (bound of index j). Analytical solution.

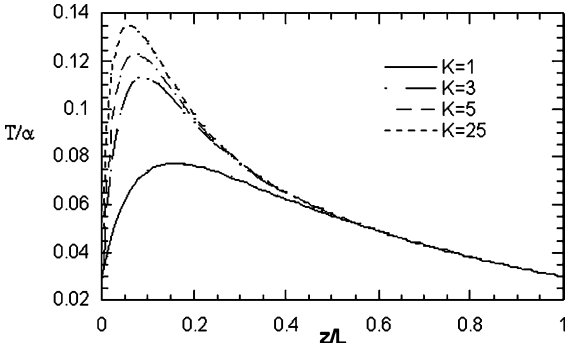

Fig. 3. Dimensionless outer surface temperature along the drum for several values of K (bound of index i). Analytical solution.

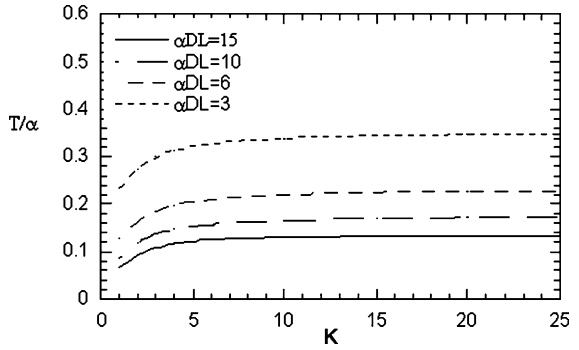

Fig. 4. Dimensionless outer surface temperature versus K (bound of index i) for several values of the product αDL. Analytical solution.

other hand, the dynamics of the system becomes slower which means that a larger number of cycles (M) must be taken into account to get the steady state cyclic solution. In conclusion, a decrease of Bi leads to an increase of M and a decrease of K that must be taken into account in order to have a convergent solution.

In a second step, the mathematical model will be solved for a realistic scenario of bakers yeast drying (Vasseur et al., 1991). These authors suggested the following empirical expression for the drying rate (with the variables in their dimensional form):

$$Q(T,X) = a_1(T-373)^{a_2} C_s^{-a_3}(1-e^{-X/a_4})^{a_5}$$

where a_i's are constants which depend on the drying material. For the bakers yeast their values are $a_1 = 539$ kW/m^2, $a_2 = 1.24$, $a_3 = 0.17$, $a_4 = 1.24$ and $a_5 = 1.45$. A typical single drum dryer is assumed with external diameter of the drum equal to 0.5 m and thickness of the wall 2 cm. The material to be dried is already preheated close to its boiling temperature and it is instantaneously applied over the drum surface. The fraction of the drum surface which is covered by the material is $p = 0.72$. The following simulations are done for initial moisture content $X_0 = 4$, rotation speed $f = 4$ rpm (it is noted that $u = 2\pi Rf$ where R is the radius of the drum), specific load $C_s = 0.03$ kg dry matter/m^2 and vapor temperature $T_v = 130$ °C. It is also assumed that the resistance to heat transfer from the condensing vapor to the drum is very small so $Bi = \infty$. Although this assumption is not realistic, it can be used to assess the effect of thermal inertia. In the experiments of Vasseur et al. (1991a) where the actual Bi varied around the drum dryer, it was shown that the temperature of the inner surface of the drum was almost constant. This means that the actual heat transfer problem is equivalent to the case where $Bi = \infty$ and an effective vapor temperature is used instead of the real one. The latter problem is actually what is solved in the present work.

The simulation of the drum dryer performance under the above conditions is done using 50 discretization points. A poor discretization becomes evident through oscillations of Q_i's close to $x = 0$ where the flux is high. Increasing the number of discretization points or alternatively using a non-uniform grid with more points close to $x = 0$ always leads to a smooth distribution of the flux. A value of $M = 10$ is enough for the particular problem to ensure periodicity in time. The temperature difference between the external surface of the wall and the condensing steam along the inside drum periphery is shown in Fig. 5. The exact result is that taken using $K = 20$ to account properly for thermal inertia. For comparison, Fig. 5 also includes the results for $K = 1$ (uniform temperature approximation), $K = 3$ and the quadratic polynomial approximation developed in the present work. The $K = 1$ solution underpredicts considerably the temperature difference since the high initial flux (proportional to the plotted temperature difference) cannot be properly computed when the temperature distribution across the wall thickness is ignored. Increasing K, the result converges to the exact solution downside. On the other hand, the polynomial model overpredicts the temperature difference showing a sudden initial jump. It is noteworthy that whereas the $K = 3$ and the polynomial approximations are of the same order (both use 3 terms of expansion to represent the temperature distribution across the wall), they give quite different results due to the different basis functions (eigenfunctions of the operator versus polynomials). Despite their different results, the two approximations are comparable in terms of accuracy. The small discontinuity in the slope of the curve for $K = 20$ at length equal to 1.13 m corresponds to the flux discontinuity at the removal point of the material. Evidently, only the $K = 20$ approximation is capable to capture this discontinuity.

From a practical point of view, the most important outcome of the simulation effort is the prediction of the final moisture X_f. The moisture distributions which correspond to the temperature distributions of Fig. 5,

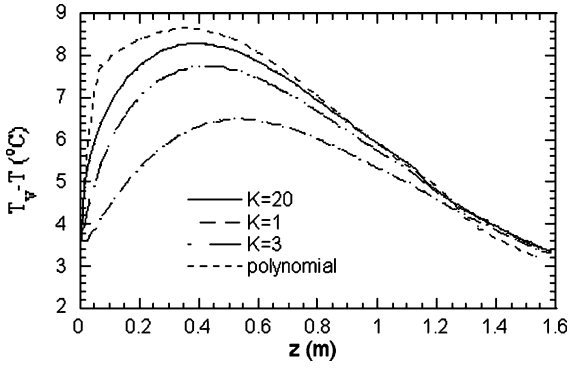

Fig. 5. Temperature difference ΔT (°C) between the condensing vapor and the outer surface of the drum along the drum surface. Comparison between the numerical solution employing several values of K and the polynomial approximation approach.

are shown in Fig. 6. The scale is logarithmic in order to exaggerate the differences in the region of low moisture. Initially, all the models follow the same moisture curve but soon differences arise among them which progressively increase along the drum periphery. The truncated ($K = 1$ and 3) approximations underpredict the moisture content, leading to a final moisture 20% smaller than the value of the exact solution, whereas the polynomial approximation overpredicts it. While the polynomial approximation is comparable to the $K = 3$ solution in terms of temperature, it is inferior in terms of moisture. The above analysis showed that only the use of the exact solution approach, with enough terms, can ensure the accuracy of the results.

In order to demonstrate the use of the model for a parametric analysis, the effect of varying the thickness of the drum wall (in a realistic range of values) on moisture distribution is shown in Fig. 7. By reducing the wall thickness from 2 to 1 cm, a 35% decrease of the final moisture X_f is achieved. The convergence of the final moisture X_f to its exact value as the number K of the eigenfunctions increases, is shown in Fig. 8 for two different values of the wall thickness. Evidently, the number of K terms needed for an accurate result depends on the particular conditions of the process. Here, for the thinner wall the thermal inertia is smaller so the convergence is achieved with a smaller K. In all cases under realistic conditions, K does not need to exceed 30.

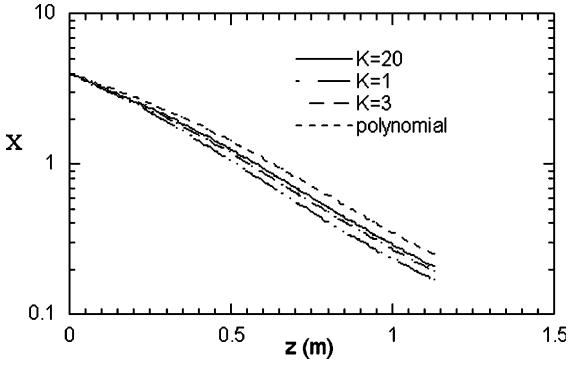

Fig. 6. Evolution of the moisture content along the drum. Comparison between the numerical solution employing several values of K and the polynomial approximation approach.

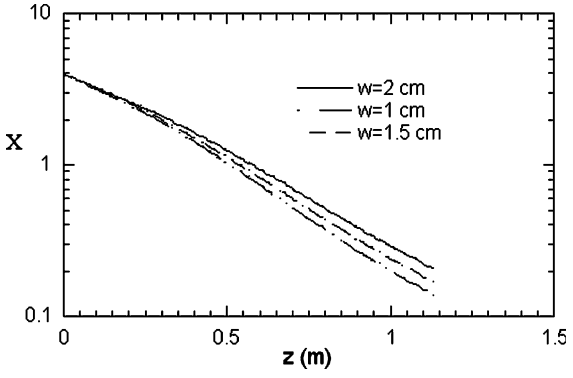

Fig. 7. Effect of the drum wall thickness, w, on the evolution of moisture content, X, along the drum.

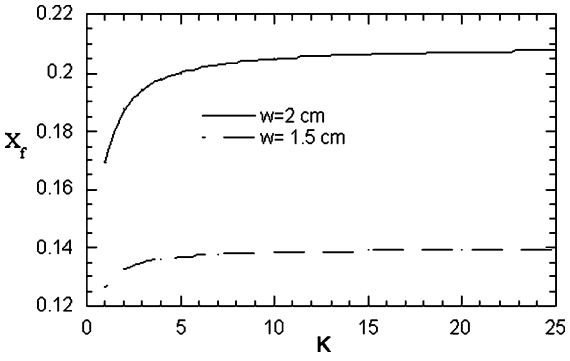

Fig. 8. The convergence of final moisture content X_f as the number of i terms increases for two values of the drum wall thickness.

The present steady state mathematical model can be used for design and optimization of the process and also for control. In order to show this capability, the final moisture content of the product is displayed in Fig. 9 as a function of the rotation speed f and vapor temperature T_v. Although the analysis includes a major simplification since C_s is assumed constant (it should be a function of f and T_v through a fluid dynamics submodel), it is yet enough to demonstrate the idea. Assuming a change of steam pressure and of the corresponding temperature T_v, the model must be solved to find the new rotation speed f that ensures that the product final moisture remains unchanged. This corresponds to the construction of the iso-moisture curves in Fig. 9.

The present implicit formulation of the mathematical problem makes it ideally suited for the above design purposes. Using instead a direct method of solution, the whole model should be solved iteratively until the computed X_f becomes equal to the desired value. This outer iteration loop is not needed by the present algorithm since the desired X_f value can be directly

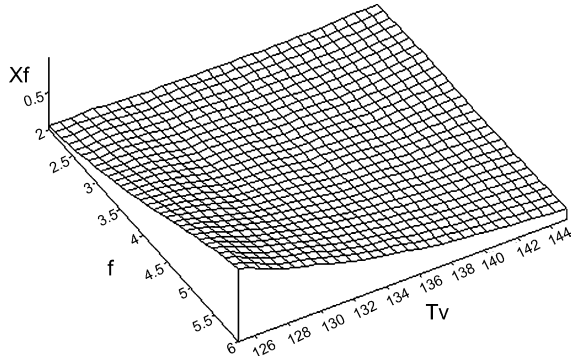

Fig. 9. Dependence of the final moisture content, X_f, from the vapor temperature, T_v (°C), and the rotation frequency, f (rpm).

incorporated in the existing Newton–Raphson code without increasing the computational cost. In this case, the unknown in the Newton–Raphson procedure is a control variable (e.g. T_v or f) instead of X_f.

8. Conclusions

The purpose of the present work is to examine the effect of the thermal inertia of the drum wall in steady state (cyclic) drum drying of food material. In order to make this effect explicit, the 2D PDE of heat transfer is transformed to an 1D integral equation which can be solved directly for the surface temperature at the cyclic steady state. A numerical approach is developed for the solution of the integral equation. The present calculations show that the effect of the drum wall thermal inertia is significant in typical drum dryers and ignoring it can lead to erroneous results. In general, the effect of thermal inertia decreases as the thickness of the wall decreases and as the drying rate decreases. The mathematical framework developed here for the solution of the heat transfer model of drum drying can be incorporated into a more global drum drying model leading to a powerful simulation tool for industrial drum dryers.

References

Abchir, R., Vasseur, J., & Trystram, G., (1988). Modelisation and simulation of drum drying. In *Proceedings of the sixth international drying symposium, Versailles, France*.

Anastasiades, A., Thanou, S., Loulis, D., Stapatoris, A., & Karapantsios, T. D. (2002). Rheological and physical characterization of pregelatinized maize starches. *Journal of Food Engineering, 52*, 57–66.

Bonazzi, C., Dumoulin, E., Raoult-Wack, A., Berk, Z., Bimbenet, J. J., Courtois, F., Trystram, G., & Vasseur, J. (1996). Food drying and dewatering. *Drying Technology, 14*(9), 2135–2170.

Crank, J. (1975). The mathematics of diffusion (2nd ed., pp. 129–135). London: Oxford University Press.

Daud, W. R. b. W. (1986). Calendering of non-Newtonian fluids. *Journal of Applied Polymer Science, 31*, 2457–2465.

Daud, W. R. b. W., & Armstrong, W. D. (1987). Pilot plant study of the drum dryer. In A. S. Mujumdar (Ed.), *Drying '87* (pp. 101–108). New York: Hemisphere Publishing Co.

Daud, W. R. b. W., & Armstrong, W. D. (1988). Conductive drying characteristics of gelatinized rice starch. *Drying Technology, 6*(4), 655–674.

Falagas, S. (1985). *Drying agricultural products* (in Greek) (pp. 80–83). Athens: ELKEPA.

Fritze, H. (1972). The use of drum dryers in the human food industry. In *International symposium of heat and mass transfer problems in food engineering, Wageningen, The Netherlands* (pp. 1–23).

Fritze, H. (1973a). Dry gelatinized produced on different types of drum dryers. *Industrial and Engineering Chemistry, Process Design and Development, 12*(2), 142–148.

Fritze, H. (1973b). Problems of heat and mass exchange at the manufacturing of foodstuffs on drum dryers. *Die Starke, 25*(7), 244–249.

Gardner, A. W. (1971). Industrial drying (pp. 220–242). London: Leonard Hill Books.

Gavrielidou, M. A., Vallous, N. A., Karapantsios, T. D., & Raphaelides, S. N. (2002). Heat transport to a starch slurry gelatinizing between the drums of a double drum dryer. *Journal of Food Engineering, 54*(1), 45–58.

Kalogianni, E., Xinogalos, V., Karapantsios, T. D., & Kostoglou, M. (2002). Effect of feed concentration on the production of pregelatinized starch in a double drum dryer. *Lebensmittel-Wissenschaft und -Technology, 35*(8), 703–714.

Kozempel, M. F., Sullivan, J. F., Craig, J. C., & Heiland, W. K. (1986). Drum drying potato flakes—a predictive model. *Lebensmittel-Wissenschaft und -Technology, 19*, 193–197.

Moore, J.G., (1995). Drum dryers. In A. S. Mujumdar (Ed.), *Handbook of industrial drying, Vol. 1* (2nd ed.) (pp. 249–262). Marcel Dekker Inc.

Nissan, A. H., & Hansen, D. (1960). Heat and mass transfer transients in cylinder drying. I. Unfelted cylinders. *AIChE Journal, 6*(4), 606–611.

Ozisik, M. N. (1989). Boundary values problem of heat conduction (1st ed., pp. 301–307). New York: Dover.

Press, W. H., Teukolsky, S. A., Vetterling, W. T., & Flannery, B. P. (1992). Numerical recipes (2nd ed., pp. 701–716). New York: Cambridge University Press.

Trystram, G., Meot, J. M., Vasseur, J., Abchir, F., & Couvrat-Desvergnes, B. (1988). Dynamic modeling of a drum dryer for food products. In *Proceedings of the sixth international drying symposium, Versailles, France*.

Trystram, G., & Vasseur, J. (1992). The modeling and simulation of a drum dryer. *International Chemical Engineering, 32*(4), 689–705.

Vallous, N. A., Gavrielidou, M. A., Karapantsios, T. D., & Kostoglou, M. (2002). Performance of a double drum dryer for producing pregelatinized maize starches. *Journal of Food Engineering, 51*, 171–183.

Vasseur, J., Abchir, F., & Trystram, G. (1991a). Modelling of drum drying. In A. S. Mujumdar, & I. Filkova (Eds.), *Drying '91* (pp. 121–129). Amsterdam: Elsevier Applied Science Publishers.

Vasseur, J., Kabbert, R., & Lebert, A. (1991b). Kinetics of drying in drum drying. In A. S. Mujumdar, & I. Filkova (Eds.), *Drying '91* (pp. 292–300). Amsterdam: Elsevier Applied Science Publishers.

Vlachos, N. A., & Karapantsios, T. D. (2000). Water content measurement of thin sheet starch products using a conductance technique. *Journal of Food Engineering, 46*(2), 91–98.